

## Josephson vortices as flexible waveguides for terahertz waves

D. R. Gulevich,<sup>1,2,a)</sup> Sergey Savel'ev,<sup>1,2</sup> V. A. Yampol'skii,<sup>2,3</sup> F. V. Kusmartsev,<sup>1</sup> and Franco Nori<sup>2,4</sup>

<sup>1</sup>Physics Department, Loughborough University, Leicestershire LE11 3TU, United Kingdom

<sup>2</sup>Advanced Science Institute, The Institute of Physical and Chemical Research (RIKEN), Wako-shi, Saitama 351-0198, Japan

<sup>3</sup>Usikov Institute for Radiophysics and Electronics, Ukrainian Academy of Science, Kharkov 61085, Ukraine

<sup>4</sup>Center for Theoretical Physics, Department of Physics, University of Michigan, Ann Arbor, Michigan 48109, USA

(Received 29 January 2008; accepted 19 July 2008; published online 23 September 2008)

We propose using the Josephson vortices (fluxons) as adjustable and malleable waveguides of electromagnetic radiation. Our theoretical and numerical calculations show that electromagnetic waves can propagate along the Josephson vortices and always follow the vortex lines. By changing external parameters, such as electric currents or magnetic fields, the shape and configuration of the guiding vortex lines can be controlled. We describe the design of a multifunctional three-terminal device that controls the transmission (redirecting or splitting) of a beam of electromagnetic waves.

© 2008 American Institute of Physics. [DOI: 10.1063/1.2979714]

### I. INTRODUCTION

The recent growing interest in terahertz science and technology is due to many applications.<sup>1,2</sup> The terahertz gap is still hard to reach for both electronic and optical devices. Numerous groups are designing sources and detectors of terahertz radiation.<sup>1,2</sup> Several competing approaches for developing terahertz sources include optical lasers, quantum cascade lasers, solid state, and superconducting devices.<sup>1-4</sup> Less studies have been devoted to the guiding and filtering of terahertz waves. Several works on terahertz waveguiding have used conventional structures, such as metal tubes<sup>5</sup> and wires,<sup>6</sup> plastic ribbons,<sup>7</sup> and dielectric fibers.<sup>8</sup> However, the mechanical and elastic properties of these systems limit their application for multiterminal terahertz devices that involve fast switching between different ports.

Here we focus our attention to devices based on either artificial contacts between two superconductors (Josephson contacts) or intrinsic Josephson junctions in layered superconductors. Superconducting Josephson junctions are considered as promising systems for developing tunable sources and detectors of high-frequency (subterahertz and terahertz) electromagnetic radiation. For instance, integrated subterahertz receivers based on low-temperature Josephson junctions have been realized.<sup>4</sup> Detecting far-field radiation emitted from a high- $T_c$  superconductor stack has been recently achieved.<sup>9</sup> An indication of terahertz emission by the vortex flow in stacked  $\text{Bi}_2\text{Sr}_2\text{CaCu}_2\text{O}_{8+x}$  intrinsic Josephson junctions has also been reported.<sup>10</sup> Terahertz and subterahertz electromagnetic waves propagating in long Josephson junctions are called the Josephson plasma waves.<sup>11</sup> An important property of the Josephson plasma waves is the gap in their energy spectrum: in the absence of an external constant magnetic field, the Josephson plasma waves can propagate only if their frequency is above the so-called Josephson plasma frequency  $\omega_p$ . Both for conventional and intrinsic junctions

in high- $T_c$  superconductors,  $\omega_p$  lies in the subterahertz frequency range;<sup>12</sup> thus, the Josephson plasma waves are potentially important for applications.<sup>13</sup> Although the use of conventional low temperature superconductors is limited to below 1 THz by the superconducting gap, high temperature layered superconductors, including  $\text{Bi}_2\text{Sr}_2\text{CaCu}_2\text{O}_{8+x}$  and  $\text{YBaCuO}$ , lift this frequency limit to over 10 THz.<sup>14</sup>

When external magnetic fields are applied, the Josephson vortices (JVs) can penetrate inside a Josephson junction. Vortices locally change the properties of a Josephson junction, allowing the propagation of plasma waves with frequency smaller than the plasma frequency  $\omega_p$ . Here we suggest the use of *vortices as flexible waveguides* and make a proposal of devices that integrate the functionality of a filter, a beam splitter, and/or a redirector of electromagnetic waves. Section II introduces general issues on the propagation of electromagnetic waves along a Josephson vortex used as a waveguide. In Sec. III we describe three-terminal devices that control the propagation of the Josephson plasma waves and present numerical simulations of the two-dimensional (2D) sine-Gordon equation. In Sec. IV we describe a possible experimental design of a three-terminal device. Section V presents some concluding remarks.

### II. PROPAGATION OF THE JOSEPHSON PLASMA WAVES ALONG A JOSEPHSON VORTEX

Formally, the Josephson vortices are soliton solutions of the nonlinear sine-Gordon equation, while plasma waves are linearized wave solutions of it. In the absence of magnetic fields, the spectrum of the Josephson plasma waves can be described by  $\omega = (1+k^2)^{1/2}$  (here we work with normalized units where lengths are normalized to the Josephson penetration length  $\lambda_J$ , frequency is normalized to the Josephson plasma frequency  $\omega_p$ , velocities are normalized to the Swihart velocity  $\bar{c} = \lambda_J \omega_p$ , which is the characteristic velocity of propagation of electromagnetic waves in a Josephson junction). Here  $k$  stands for the modulus of the wave vector.

<sup>a)</sup>Electronic mail: phdrg@lboro.ac.uk.

Thus, linear Josephson plasma waves cannot propagate if their frequency  $\omega$  is smaller than 1 ( $\omega_p$  in physical units). The presence of a vortex effectively suppresses the critical current density and allows propagation of the Josephson plasma waves below the plasma frequency with linear dispersion  $\omega=k$ .

Consider a long Josephson junction located in the  $xy$ -plane, i.e., the  $z$ -axis is perpendicular to the junction plane. The sine-Gordon equation for the gauge-invariant phase difference  $\varphi$  reads (e.g., Ref. 15)

$$\ddot{\varphi} - \Delta\varphi + \sin\varphi = 0. \quad (1)$$

Here, the coordinates  $x$  and  $y$  are normalized by the Josephson length  $\lambda_J$ , and the time  $t$  is normalized by  $\omega_p^{-1}$ . Let

$$\varphi(x, y, t) = \varphi_{JV}(x) + \psi(x, y, t),$$

where

$$\varphi_{JV}(x) = 4 \arctan e^x$$

is a stationary phase distribution produced by a JV and  $|\psi| \ll 1$ . We seek a solution of the form

$$\psi(x, y, t) = \chi(x)\exp(i\omega t -iky)$$

for the Josephson plasma waves of frequency  $\omega > 0$  propagating along the JV. When keeping only the linear terms in  $\psi$ , the wave amplitude  $\chi$  obeys an equation analogous to the one-dimensional Schrödinger equation with a reflectionless potential  $-1/\cosh^2 x$

$$\frac{d^2\chi}{dx^2} + 2\left\{\frac{\omega^2 - k^2 - 1}{2} + \frac{1}{\cosh^2 x}\right\}\chi = 0. \quad (2)$$

Some of the solutions of Eq. (2) are of the form

$$\chi_q(x) = a(\tanh x + iq)e^{-iqx}$$

and are associated with the continuum spectrum  $\omega = (1 + k^2 + q^2)^{1/2}$ . These are waves running at an angle  $\theta = \arctan(k/q)$  with respect to the Josephson vortex. The other solution

$$\chi_{\text{loc}}(x) = \frac{a}{\cosh x}$$

corresponds to a wave

$$\psi(x, y, t) = \chi_{\text{loc}}(x)\exp(i\omega t -iky)$$

localized in the  $x$  direction and running along a Josephson vortex line. Substituting the solution  $\chi_{\text{loc}}(x)$  to Eq. (2) we obtain the linear dispersion relation  $\omega=k$ . This branch of the spectrum is gapless, which is not the case for conventional Josephson plasma waves. Similar gapless spectrum of electromagnetic waves was obtained for an array of vortices 40 years ago in Ref. 16.

Note that the waves with  $\omega < 1$  may only propagate along a Josephson vortex and always follow the vortex line. Thus, a vortex behaves as a flexible waveguide for such Josephson plasma waves. This opens an opportunity for designing classes of devices that employ the Josephson vortices to guide and filter electromagnetic radiation. To demonstrate

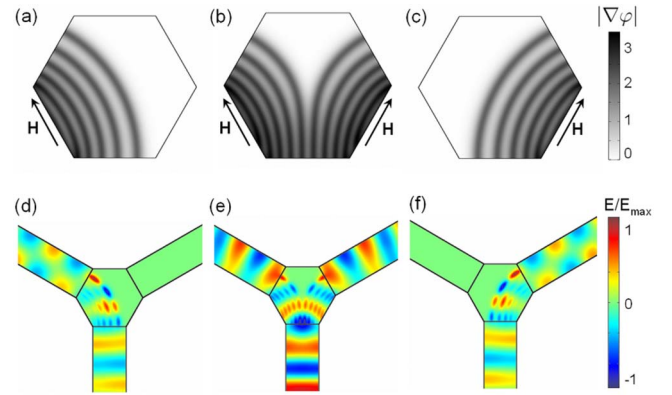


FIG. 1. (Color online) [(a)–(c)] Vortex configurations in a hexagonal Josephson junction with each side equal to 20 Josephson penetration lengths  $\lambda_J$ . The color scale denotes the magnetic field density given by the gradient of the superconducting phase difference  $|\nabla\varphi|$ . [(d)–(f)] Propagation of the Josephson plasma waves with frequency  $\omega=0.32$ . The plasma frequency of the Josephson transmission lines is  $\tilde{\omega}_p=0.2\omega_p$ , where  $\omega_p$  is that of the hexagonal junction. The width of the attached Josephson transmission lines is  $W=20$  in normalized units. The damping is absent. [(d)–(f)] correspond to the vortex configurations (a)–(c). The color scale depicts the relative amplitude of the plasma waves as a ratio of the transverse electric field  $E$  to its maximal value  $E_{\text{max}}$  for each simulation. (d) and (e) show mode transfers from planar waves to alternating wave mode in the upper branches. Numerical solutions showing the spatiotemporal evolution of the waves are available online (Ref. 17).

this novel concept here we focus our attention on a three-terminal device for controlling electromagnetic waves.

### III. SPLITTER OF THE JOSEPHSON PLASMA WAVES

Because the arrangements of the Josephson vortices can be controlled by an external magnetic field or electric currents, it is possible to change the direction of propagating the Josephson plasma waves by tuning the external parameters. We have performed numerical simulations that demonstrate the guiding of electromagnetic waves by several configurations involving a number of vortices. A few of these results are available as online videos in Ref. 17. To control the Josephson plasma waves we would like to have a system where the arrangement and orientation of vortices are effectively tuned by a magnetic field, so that the orientation of the vortices can be controlled. We will call this system a *wave splitter*. The splitter can be realized as a hexagonal-shaped 2D Josephson junction as shown in Fig. 1. Different stable configurations can be initiated by applying an external magnetic field to different edges of the hexagon. Depending on the orientation of the vortex arrangement, electromagnetic waves incoming from, say, the bottom edge of a hexagon will follow the JV lines and will be redirected according to the orientation of the Josephson vortices inside.

Using a finite element software package COMSOL MULTIPHYSICS 3.2A we have performed numerical simulations of the 2D sine-Gordon equation [Eq. (1)] for a hexagonal splitter, as shown in Fig. 1. First, stable arrangements of vortices have been calculated for the cases when a magnetic field is applied to different edges. A magnetic field applied to a particular edge of the hexagon forces vortices to penetrate inside it “linking” two adjacent edges [see, e.g., Fig. 1(a)]. We used

the following Neumann boundary conditions (see, e.g., Ref. 15):

$$\mathbf{n} \cdot \nabla \varphi = 0$$

for boundaries with no magnetic field and

$$\mathbf{n} \cdot \nabla \varphi = \mathbf{n} \cdot (\mathbf{H} \times \mathbf{e}_z)$$

for the boundary with applied magnetic field  $\mathbf{H}$  [see Figs. 1(a)–1(c)]. Here  $\mathbf{H}$  is normalized by  $H_0 = \lambda_J j_c$ , where  $\lambda_J$  and  $j_c$  are the Josephson penetration length and critical current density of the hexagonal contact, correspondingly, and  $\mathbf{e}_z$  is a unitary vector.

After the stable configurations of vortices are found, we have simulated the propagation of linear Josephson plasma waves through each of them. We send a beam of the Josephson plasma waves and look for the transmission of waves through the system after its dynamics is stabilized. As shown in Fig. 1 and in the numerical solution animations in Ref. 17, the incoming beam of plane waves enters through the bottom transmission line that is coupled to the bottom boundary of the hexagon. We model the transmission line by a long Josephson junction with a plasma frequency  $\tilde{\omega}_p$  lower than the plasma frequency in the hexagonal junction  $\omega_p$ . This allows the propagation of waves of frequency  $\omega$  in the transmission line, but not in the hexagon itself if the vortices are absent and  $1 > \omega > \tilde{\omega}_p / \omega_p$ . Propagation of waves in the Josephson transmission lines can be described by the linear equation for the electric field component  $E$

$$\ddot{E} - \Delta E + \sigma^2 E = 0$$

with  $\sigma = \tilde{\omega}_p / \omega_p$ , ratio of plasma frequencies in the Josephson transmission lines and in the hexagonal junction, and

$$\ddot{E} - \Delta E + \cos[\varphi(x, y)]E = 0$$

in the hexagonal junction, where  $\varphi(x, y)$  describes the stationary configuration of the Josephson vortices calculated numerically from the 2D sine-Gordon equation [Figs. 1(a)–1(c)]. We use continuous boundary conditions for the electric field components to link the hexagon with the transmission lines. The incident beam of electromagnetic waves in the lower transmission line [see Figs. 1(d)–1(f)] had the form of the plane wave  $E(x, y, t) = \sin(\omega t - ky)$  with amplitude 1 and the wave vector  $k = (\omega^2 - \sigma^2)^{1/2} > 0$ . Solving the time-dependent linear problem of wave propagation through the stable vortex configurations, we obtain the distribution of electric field component  $E$  for transverse electric waves in the Josephson junctions [Figs. 1(d)–1(f)]. One can see that the peak concentrations of the electric field in the hexagon tend to follow each vortex, as was described in Sec. II.

We have quantitatively studied the transmission of the Josephson plasma waves through the configuration of the Josephson vortices shown in Fig. 1(a). The transmission coefficient  $T$  was defined as the ratio of the input and output energy fluxes

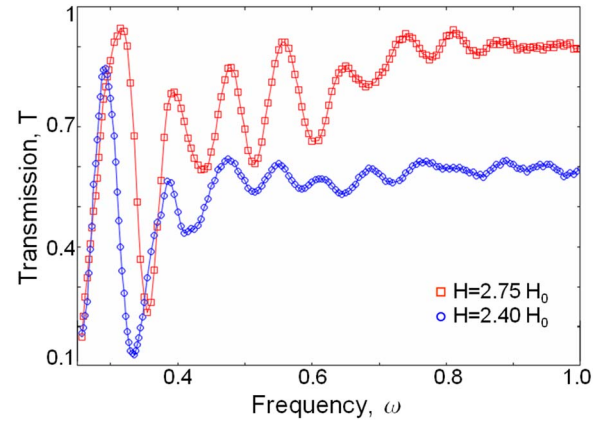


FIG. 2. (Color online) Dependence of the transmission coefficient  $T$  on the plasma wave frequency  $\omega$ . The peaks and dips are related to the matching of the plasma wavelength to the length of the vortex lines. The plasma frequency of the Josephson transmission lines is  $\tilde{\omega}_p = 0.2\omega_p$ , where  $\omega_p$  is that of the hexagonal junction.

$$T = \frac{E_{\text{out}}(t + \Delta t) - E_{\text{out}}(t)}{\int_t^{t+\Delta t} P_{\text{in}} dt}$$

at some time  $t$ , long enough for the dynamics in the hexagonal junction to have stabilized. Here  $E_{\text{out}}(t)$  is the total energy accumulated in the output transmission line

$$E_{\text{out}}(t) = \iint \left[ \frac{\dot{E}^2}{2} + \frac{(\nabla E)^2}{2} + \frac{\sigma^2 E^2}{2} \right] dx dy,$$

where integration is over the domain of the Josephson transmission line and  $P_{\text{in}}$  is the input energy flux carried by the incident plane wave. Using the plane wave in the forms  $E(x, y, t) = \sin(\omega t - ky)$  and  $\Delta t = 2\pi/\omega$ , the integral

$$\int_t^{t+\Delta t} P_{\text{in}} dt = \pi kW,$$

where  $W = 20$  is the normalized width of the transmission line.

The frequency dependence  $T(\omega)$  for the configuration [Fig. 1(a)] at different values of the magnetic field is shown in Fig. 2: it exhibits oscillations associated with the matching of the wave vector  $k$  with the full length  $L$  of each vortex line,  $k = k_n \equiv \pi n / L$  with integer  $n$ . Thus, the peaks of transmission are at frequencies

$$\omega_n = \sqrt{\sigma^2 + k_n^2}. \quad (3)$$

For lower frequencies (smaller wave vectors) the matching of the longest vortex is the most pronounced. For example, the first four peaks for the top (red) curve in Fig. 2 can be associated with the resonance frequencies  $n = 3, 4, 5, 6$  that occur on the longest vortex with  $L \approx 37$ . One sees that the peaks occur at  $\omega_3 = 0.32$ ,  $\omega_4 = 0.39$ ,  $\omega_5 = 0.47$ , and  $\omega_6 = 0.55$ . At lower frequencies, the amplitude of oscillations is large and related to the matching of the waves to the longest vortex, whereas for higher frequencies the amplitude of oscillations decays due to the interference of waves propagating through several vortex lines [see Fig. 2].

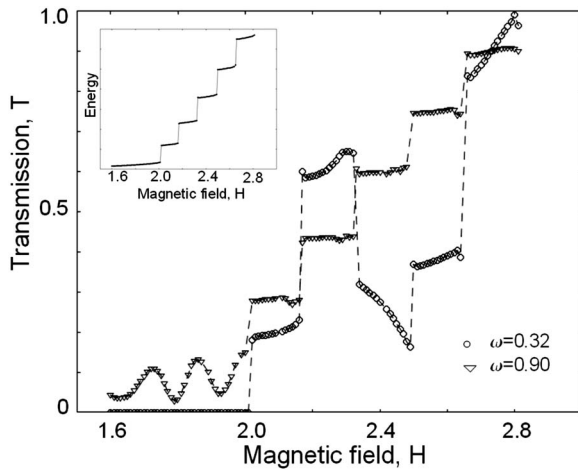


FIG. 3. Dependence of the transmission coefficient  $T$  on the applied magnetic field  $H$  for two fixed frequencies,  $\omega=0.32$  and  $\omega=0.90$ . The abrupt steps are associated with the penetration of a new vortex when a magnetic field is increased. The associated change in energy of the arrangement of vortices in the hexagonal Josephson contact is shown in the inset.

Increasing the magnetic field  $H$  applied to one of the edges can abruptly change the vortex configuration when a new vortex penetrates. This results in a series of transmission steps observed in our numerical simulations and is shown in Fig. 3. Increasing  $H$  not only increases  $T$  but, surprisingly, may also lead to a drop in  $T(H)$ . The latter effect is associated with changing the length of the vortices away from the resonant matching condition [Eq. (3)]. This is more pronounced for lower frequencies, as seen in the inset of Fig. 2.

Note that the device can also change the propagation mode in the transmission lines, as seen in Figs. 1(d) and 1(f) and Fig. 1(e). Depending on the vortex configuration, a wave with zero transverse wave vector propagating in an input transmission line can transform into a wave with nonzero transverse wave vector for Figs. 1(d) and 1(f) or to the same mode, Fig. 1(e). This offers the possibility of using this device as a “mode changer.”

#### IV. POSSIBLE REALIZATION OF A THREE-TERMINAL MULTIFUNCTIONAL DEVICE

A Josephson plasma wave splitter can be implemented as shown in Fig. 4. Three of the six edges of the hexagonal junction play the role of terminals (ports  $P_1$ ,  $P_2$ , and  $P_3$ ) where the Josephson plasma waves can enter or exit. In particular, the conventional waveguides or long Josephson junctions (Josephson transmission lines) with the Josephson plasma frequency  $\tilde{\omega}_p$  lower than  $\omega_p$  in the hexagon can be attached to these terminals. In this case, the Josephson plasma waves with frequencies between  $\tilde{\omega}_p$  and  $\omega_p$  can propagate along the Josephson transmission lines but are reflected by the hexagonal junction. The other three edges of the hexagon are used for injecting the Josephson vortices inside the system. This can be done by applying electric currents flowing in thin electrode strips attached to the edges, as shown in Fig. 4. If the thickness of the structure is much smaller than the width of the electrodes, the magnetic field is mainly localized between the top and bottom electrodes. Thus, an electric current flowing in two parallel electrodes

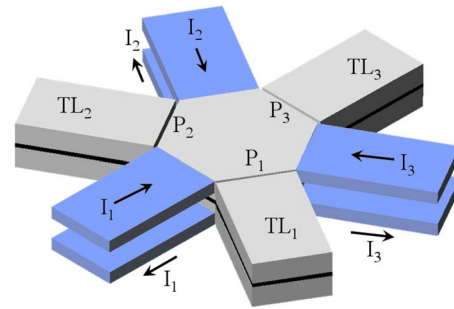


FIG. 4. (Color online) Schematic of a three-terminal electromagnetic wave controller based on a hexagonal-shaped Josephson junction. The three terminals or ports,  $P_1$ ,  $P_2$ , and  $P_3$ , are used to input/output electromagnetic waves by means of the attached transmission lines  $TL_1$ ,  $TL_2$ , and  $TL_3$  (shown in gray). The currents  $I_1$ ,  $I_2$ , and  $I_3$  flowing along the top and bottom parallel electrodes (shown in blue), connected to the edges of the hexagonal junction, control the value of the magnetic field.

induces a magnetic field on only one edge of the hexagon and provides a negligible contribution to the magnetic field on all other edges. This results in the penetration of vortices through the edge confined between electrodes with the current. Therefore, we can manipulate the configuration of vortices with the external currents  $I_1$ ,  $I_2$ , and  $I_3$  [see Figs. 1(a)–1(c)]. For instance, when applying current  $I_1$  we can link ports  $P_1$  and  $P_2$  by the Josephson vortex lines [Fig. 1(a)]. By properly adjusting currents  $I_1$ ,  $I_2$ , and  $I_3$  this device links any ports, including situations where more than two ports are linked to each other [e.g., Fig. 1(b)]. According to our numerical calculations with 2D sine-Gordon equation, the typical switching time between configurations [Figs. 1(a) and 1(c)] is determined by both damping and the characteristic size of the system, and it lies in the range of nanoseconds or faster.

The Josephson plasma waves propagating in the transmission line  $TL_1$  can be directed to either  $TL_2$  by applying current  $I_1$ , or toward  $TL_2$  by applying current  $I_3$  [see Figs. 1(a), 1(c), 1(d), and 1(f)]. Thus, the device can be used to redirect terahertz radiation coming from port  $P_1$  to either  $P_2$  or  $P_3$  by guiding the Josephson plasma waves along the Josephson vortices. If we simultaneously apply currents  $I_1$  and  $I_3$ , the same device can be used to split a beam of terahertz radiation into two beams propagating in  $TL_2$  and  $TL_3$ . This is shown in Figs. 1(b) and 1(e). Thus, beams of the Josephson plasma waves can be effectively controlled by currents  $I_1$ ,  $I_2$ , and  $I_3$ .

#### V. CONCLUSION

We have shown that the Josephson vortices can act as waveguides for low frequency Josephson plasma waves that otherwise cannot propagate and proposed a three-terminal device that can split, redirect, and filter waves. The device can be tuned by external currents and can switch quickly between different operating regimes. Because *no* mechanical parts are involved, such devices are expected to be more reliable compared to their mechanical analogs and could be integrated in one chip with other superconducting devices. Analogous physical systems similar to the proposed splitter of the Josephson plasma waves were discussed earlier in the

literature: electron waveguide  $Y$  switches,<sup>18</sup> atomic double waveguides,<sup>19</sup> soliton splitters,<sup>20</sup> and plasmon-polariton  $Y$  splitters.<sup>21</sup> Standing alongside with them, the splitter of the Josephson plasma waves can be well controlled by electric currents and may find applications in subterahertz or terahertz technology.

## ACKNOWLEDGMENTS

We would like to thank A. Ustinov for instructive correspondence about the practical importance of terahertz devices and B.A. Ivanov for the stimulating discussions. We acknowledged partial support from the NSA, LPS, ARO, NSF (Grant No. EIA-0130383), JSPS-RFBR (Grant No. 06-02-91200), JSPC-CTC program, and MEXT (Grant-in-Aid No. 18740224). Also, we acknowledge support from the EPSRC via Grant Nos. EP/D072581/1, EP/E042589/1, and EP/F005482/1 and ESF network program “AQDJJ.”

<sup>1</sup>See, e.g., the special issue in *Philos. Trans. R. Soc. London, Ser. A* **362**(1815) (2004).

<sup>2</sup>See, e.g., M. Tonouchi, *Nat. Photonics* **1**, 97 (2007); B. Ferguson and X.-C. Zhang, *Nat. Mater.* **1**, 26 (2002); S. Nakajima, H. Hoshina, M. Yamashita, C. Otani, and N. Miyoshi, *Appl. Phys. Lett.* **90**, 041102 (2007); A. Dobroiu, C. Otani, and K. Kawase, *Meas. Sci. Technol.* **17**, R161 (2006).

<sup>3</sup>S. Ariyoshi, C. Otani, A. Dobroiu, H. Sato, K. Kawase, H. M. Shimizu, T. Taino, and H. Matsuo, *Appl. Phys. Lett.* **88**, 203503 (2006); M. Tani, O. Morikawa, S. Matsuura, and M. Hangyo, *Semicond. Sci. Technol.* **20**, S151 (2005); M. Hangyo, M. Tonouchi, M. Tani, and K. Sakai, *LEOS '99: The IEEE Lasers and Electro-Optics Society*, 1999 (unpublished), Vol. 2, p. 629.

<sup>4</sup>V. P. Koshelets and S. V. Shitov, *Supercond. Sci. Technol.* **13**, R53 (2000); V. P. Koshelets, S. V. Shitov, A. B. Ermakov, O. V. Koryukin, L. V. Filippenko, A. V. Khudchenko, M. Yu. Torgashin, P. Yagoubov, R. Hoogeveen, and O. M. Pylypenko, *IEEE Trans. Appl. Supercond.* **15**, 960 (2005); V. P. Koshelets, P. N. Dmitriev, A. B. Ermakov, A. S. Sobolev, M. Yu. Torgashin, V. V. Kurin, A. L. Pankratov, and J. Mygind, *ibid.* **15**, 964 (2005); J. Mygind, M. R. Samuelsen, V. P. Koshelets, and A. S. Sobolev, *ibid.* **15**, 968 (2005); V. P. Koshelets, A. B. Ermakov, L. V. Filippenko, A. V. Khudchenko, O. S. Kiselev, A. S. Sobolev, M. Yu. Torgashin, P. A. Yagoubov, R. W. M. Hoogeveen, and W. Wild, *ibid.* **17**, 336 (2007); M.

Yu. Torgashin, V. P. Koshelets, P. M. Dmitriev, A. B. Ermakov, L. V. Filippenko, and P. A. Yagoubov, *ibid.* **17**, 379 (2007).

<sup>5</sup>R. W. McGowan, G. Gallot, and D. Grischkowsky, *Opt. Lett.* **24**, 1431 (1999); G. Gallot, S. P. Jamison, R. W. McGowan, and D. Grischkowsky, *J. Opt. Soc. Am. B* **17**, 851 (2000).

<sup>6</sup>K. Wang and D. M. Mittleman, *Nature (London)* **432**, 376 (2004).

<sup>7</sup>R. Mendis and D. Grischkowsky, *J. Appl. Phys.* **88**, 4449 (2000).

<sup>8</sup>S. P. Jamison, R. W. McGowan, and D. Grischkowsky, *Appl. Phys. Lett.* **76**, 1987 (2000).

<sup>9</sup>L. Ozyuzer, A. E. Koshelev, C. Kurter, N. Gopalsami, Q. Li, M. Tachiki, K. Kadowaki, T. Yamamoto, H. Minami, H. Yamaguchi, T. Tachiki, K. E. Gray, W.-K. Kwok, and U. Welp, *Science* **318**, 1291 (2007).

<sup>10</sup>M.-H. Bae, H.-J. Lee, and J.-H. Choi, *Phys. Rev. Lett.* **98**, 027002 (2007).

<sup>11</sup>Y. Matsuda, M. B. Gaifullin, K. Kumagai, K. Kadowaki, and T. Mochiku, *Phys. Rev. Lett.* **75**, 4512 (1995).

<sup>12</sup>Y. Tominari, T. Kiwa, H. Murakami, M. Tonouchi, H. Wald, P. Seidel, and H. Schneidewind, *Appl. Phys. Lett.* **80**, 3147 (2002); M. Tachiki, M. Iizuka, S. Tejima, and H. Nakamura, *Phys. Rev. B* **71**, 134515 (2005).

<sup>13</sup>S. Savel'ev, V. Yampol'skii, A. Rakhmanov, and F. Nori, *Phys. Rev. B* **72**, 144515 (2005); **75**, 184503 (2007); S. Savel'ev, A. Rakhmanov, and F. Nori, *Phys. Rev. B* **74**, 184512 (2006); **94**, 157004 (2005); **98**, 077002 (2007); S. Savel'ev, V. Yampol'skii, and F. Nori, *Phys. Rev. Lett.* **95**, 187002 (2005); S. Savel'ev, A. Rakhmanov, V. Yampol'skii, and F. Nori, *Nat. Phys.* **2**, 521 (2006); V. A. Yampol'skii, S. Savel'ev, O. V. Usatenko, S. S. Mel'nik, F. V. Kusmartsev, A. A. Krokhin, and F. Nori, *Phys. Rev. B* **75**, 014527 (2007); V. A. Yampol'skii, A. V. Kats, M. L. Nesterov, A. Yu. Nikitin, T. M. Slipchenko, S. Savel'ev, and F. Nori, *ibid.* **76**, 224504 (2007).

<sup>14</sup>E. Stepantsov, M. Tarasov, A. Kalabukhov, L. Kuzmin, and T. Claeson, *J. Appl. Phys.* **96**, 3357 (2004).

<sup>15</sup>A. Barone and G. Paternó, *Physics and Applications of Josephson Effect* (Wiley, New York, 1982).

<sup>16</sup>I. O. Kulik, *Sov. Phys. JETP* **24**, 1307 (1967); P. Leubwohl and M. J. Stephen, *Phys. Rev.* **163**, 376 (1967); A. Fetter and M. Stephen, *Phys. Rev.* **168**, 475 (1968); I. O. Kulik and I. K. Yanson, *The Josephson Effect in Superconductive Tunneling Structures* (Keter, Jerusalem, 1972).

<sup>17</sup>Animations based on numerical solutions, illustrating some of our results, are available online at <http://dml.riken.jp/waveguides>

<sup>18</sup>T. Palm, *J. Appl. Phys.* **74**, 3551 (1993); J.-O. J. Wesström, *Phys. Rev. Lett.* **82**, 2564 (1999).

<sup>19</sup>O. Zoby and B. M. Garraway, *Opt. Commun.* **178**, 93 (2000).

<sup>20</sup>D. R. Gulevich and F. V. Kusmartsev, *Phys. Rev. Lett.* **97**, 017004 (2006); *Supercond. Sci. Technol.* **20**, S60 (2007); *New J. Phys.* **9**, 59 (2007).

<sup>21</sup>F. J. Garcia-Vidal, *Nature (London)* **440**, 431 (2006); S. I. Bozhevolnyi, V. S. Volkov, E. Devaux, J.-Y. Laluet, and T. W. Ebbesen, *ibid.* **440**, 508 (2006); H. A. Atwater, *Sci. Am.* **296**, 56 (2007).